

The Intricate Structure of HH 508, the Brightest Microjet in the Orion Nebula

YA-LIN WU, LAIRD M. CLOSE, JINYOUNG SERENA KIM, JARED R. MALES, AND KATIE M. MORZINSKI
Steward Observatory, University of Arizona, Tucson, AZ 85721, USA

Published in ApJ

ABSTRACT

We present *Magellan* adaptive optics H α imaging of HH 508, which has the highest surface brightness among protostellar jets in the Orion Nebula. We find that HH 508 actually has a shorter component to the west, and a longer and knotty component to the east. The east component has a kink at 0 $^{\prime}$.3 from the jet-driving star θ^1 Ori B₂, so it may have been deflected by the wind/radiation from the nearby θ^1 Ori B₁B₅. The origin of both components is unclear, but if each of them is a separate jet, then θ^1 Ori B₂ may be a tight binary. Alternatively, HH 508 may be a slow-moving outflow, and each component represents an illuminated cavity wall. The ionization front surrounding θ^1 Ori B₂B₃ does not directly face θ^1 Ori B₁B₅, suggesting that the EUV radiation from θ^1 Ori C plays a dominant role in affecting the morphology of proplyds even in the vicinity of θ^1 Ori B₁B₅. Finally, we report an H α blob that might be ejected by the binary proplyd LV 1.

Keywords: H II regions – ISM: individual objects (Orion Nebula, HH 508, LV 1) – protoplanetary disks – stars: formation

1. Introduction

At a distance of ~ 388 pc, the Orion Nebula is the nearest high-mass star-forming region (Kounkel et al. 2017) and offers a clear view of jet irradiation and disk destruction due to strong UV radiation from OB stars (e.g., Johnstone et al. 1998; Bally & Reipurth 2001), especially in regions around the Trapezium cluster. Observations have revealed the presence of photoevaporated protoplanetary disks (proplyds) with bow-shaped ionization fronts (IFs) facing toward and cometary tails pointing away from the dominant ionizing star of the Trapezium cluster, θ^1 Ori C (O’Dell et al. 1993; O’Dell & Wen 1994; Bally et al. 1998, 2000). Over the past ~ 20 yr, hundreds of proplyds have been imaged from optical to radio wavelengths in the Orion Nebula (e.g., Bally et al. 1998; Smith et al. 2005; Ricci et al. 2008; Mann & Williams 2010; Mann et al. 2014; Eisner et al. 2016; Sheehan et al. 2016).

Proplyds are often associated with jets, many of which are short, one-sided, and bright in optical emission, such as H α , [S II], and [O III]. These compact irradiated jets are sometimes called “microjets” (Bally et al. 2000, 2006; Bally & Reipurth 2001). Bally & Reipurth (2001) suggested that the one-sided asymmetry often observed in irradiated jets likely arises from different densities of matter between the irradiated and shadowed sides of a disk. External UV radiation can more effectively remove material on the irradiated side; as a result, the jet facing the UV source can move faster than the counterjet on the shadowed side of the disk. Since the surface brightness of irradiated jets correlates with the amount of incident UV flux when the jets are optically thick to Lyman continuum radiation, jets close to an ionizing star will be more luminous. At $\sim 1''$ from the eclipsing binary θ^1 Ori B₁B₅ (Windemuth et al. 2013, and references therein), HH 508 is considered the brightest microjet in the Orion Nebula (Bally et al. 2000, 2006). In *Hubble Space Telescope* (*HST*) images, HH 508 appears one-sided and $\sim 0.5'$ in length emerging from θ^1 Ori B₂.

We note that θ^1 Ori B (BM Ori) is a hierarchical “mini-cluster” with three outer members, B₂B₃B₄, orbiting the inner binary B₁B₅ (Petr et al. 1998; Close et al. 2003, 2012, 2013). Close et al. (2013) further demonstrated that the components B₂ and B₃ also orbit each other in a nearly circular orbit with a period of ~ 300 yr. The stellar masses for components 1, 2, 3, 4, and 5 are estimated to be 6.3, 3, 2.5, 0.2, and 2.5 M_{\odot} , respectively (Vitrichenko et al. 2006; Close et al. 2013). Numerical simulations have shown that this quintuple¹ is unstable, with a very short dynamical lifetime, ~ 30 kyr (Allen et al. 2015, 2017).

This close separation between HH 508 and θ^1 Ori B₁B₅ enables excellent adaptive optics (AO) performance in that the unresolved binary can serve as the natural guide star. It is therefore possible to resolve the structure of HH 508 with ground-based telescopes. In this paper, we present H α images of HH 508 obtained with the *Magellan* adaptive optics (MagAO; Close et al. 2012; Males et al. 2014; Morzinski et al. 2014). MagAO has been fully operational on the 6.5 m Clay Telescope since 2012. With a resolution of 33 mas, we show that HH 508 has complex structure and may have been deflected by the wind and radiation from θ^1 Ori B₁B₅. In addition to HH 508, we also present multi-epoch H α images of the binary proplyd LV 1, showing that the major proplyd may have had episodic mass ejection.

2. Observations and Data Reduction

HH 508 was observed in 2016 with θ^1 Ori B₁B₅ ($V \sim 6.4$ mag) being the guide star, and LV 1 was observed in 2012, 2014, and 2016 with θ^1 Ori C ($V \sim 5.1$ mag) being the guide star. All data were taken with MagAO’s simultaneous differential imaging mode (Close et al. 2014) at 643 nm and 656 nm (H α). The 2012 data of LV 1 were previously published in Wu et al. (2013). Since HH

¹ The system might be a sextuple, as Vitrichenko & Klochkova (2004) proposed a third component in an eccentric orbit to the inner binary B₁B₅ to explain the observed radial velocity anomaly.

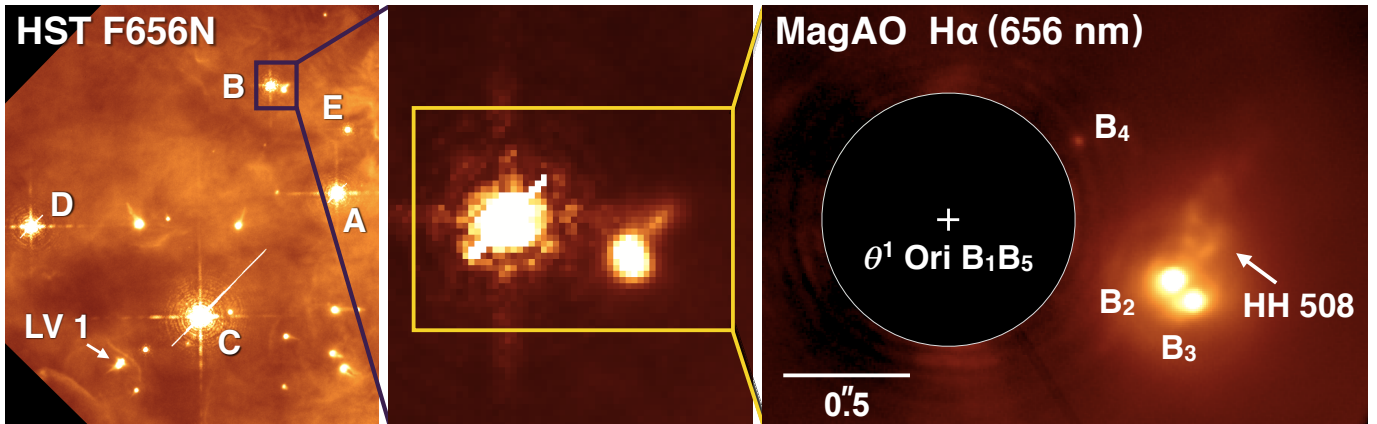


Figure 1. MagAO and *HST* $H\alpha$ images of HH 508 and the θ^1 Ori B system. We spatially resolve the complex structure of HH 508. The central $0''.5$ around B_1B_5 in the MagAO image is masked out. The *HST* image is from the program GO 5469. North is up and east is left.

Table 1
MagAO $H\alpha$ Observations of HH 508 and LV 1

Object	Date	Speed	Mode	Exposure	Guide Star	FWHM
HH 508	2016 Feb 17	990 Hz	300	$2.273 \text{ s} \times 201$	θ^1 Ori B_1B_5	33 mas
LV 1	2012 Dec 03	990 Hz	250	$10 \text{ s} \times 60$	θ^1 Ori C	40 mas
	2014 Nov 17	990 Hz	300	$7.5 \text{ s} \times 488$	θ^1 Ori C	39 mas
	2016 Jul 01	990 Hz	300	$60 \text{ s} \times 66$	θ^1 Ori C	49 mas

Table 2
Luminosities of the Trapezium OB Stars and the UV Fluxes at the Position of HH 508

Star	Angular Offset to B_2B_3 ($''$)	$\log L_{\text{bol}}$ (L_{\odot})	$\log L_{\text{EUV}}$ (L_{\odot})	EUV Flux at B_2B_3 (W m^{-2})	$\log L_{\text{FUV}}$ (L_{\odot})	FUV Flux at B_2B_3 (W m^{-2})
θ^1 Ori A	8.1	4.50	3.01	0.14	4.36	3.2
θ^1 Ori B_1B_5	1.0	3.28	-0.42	3.5×10^{-3}	3.05	10.5
θ^1 Ori C	16.9	5.40	4.81	2.1	5.16	4.6
θ^1 Ori D	20.1	4.35	2.71	1.2×10^{-2}	4.21	0.37
θ^1 Ori E	5.3	2.42	-2.85	4.7×10^{-7}	2.07	3.9×10^{-2}

508 and LV 1 are absent in the 643 nm continuum, we only present the $H\alpha$ images in this paper. Table 1 summarizes our observations. The pixel scale at $H\alpha$ is ~ 7.9 mas pix^{-1} (Close et al. 2013).

The data reduction was carried out with IRAF² (Tody 1986, 1993) and MATLAB. We subtracted the dark frame from the raw data, rotated the dark-subtracted frames so that north is up, then registered and combined the images. We removed the halo of θ^1 Ori B_1B_5 from the combined image by subtracting its azimuthal profile.

3. Results

3.1. Two Components of HH 508

Figure 1 shows the MagAO and *HST* $H\alpha$ images of the θ^1 Ori B system. Our high-resolution image reveals a two-component structure for HH 508. The west component is short, while the east component is longer, knotty, and has a kink at $\sim 0''.3$ from θ^1 Ori B_2 . The kink may

imply that the east component has been deflected by $\sim 20^\circ$ by the wind and radiation from θ^1 Ori B_1B_5 . We note that we do not see a cometary tail pointing away from B_1B_5 as mentioned by Bally et al. (2000).

The origin of the two-component structure remains puzzling. One possibility is that θ^1 Ori B_2 is a tight binary, so each component is a separate jet. Alternatively, HH 508 could be a wide and slow-moving outflow, so one or both components may be the outflow cavity walls. Unlike jets, which are collimated and launched in the innermost disk, outflows can be launched at larger disk radii or entrained by the jets. $H\alpha$ outflows have been observed in the Carina Nebula, including HH 666, HH 900, and HH 1163 (Reiter et al. 2015a, 2015b, 2016). Future spectroscopic or astrometric observations should be able to distinguish fast-moving jets from slow-moving cavity walls.

3.2. Orientation and Size of the Ionization Front

As shown in Figures 1 and 2, the bow-shaped ionization front surrounding θ^1 Ori B_2B_3 does not face toward the nearby θ^1 Ori B_1B_5 ($\sim 1''$); in contrast, it points to the distant θ^1 Ori C ($\sim 17''$). Ionizing photons from θ^1 Ori C

² IRAF is distributed by the National Optical Astronomy Observatories, which are operated by the Association of Universities for Research in Astronomy, Inc., under cooperative agreement with the National Science Foundation.

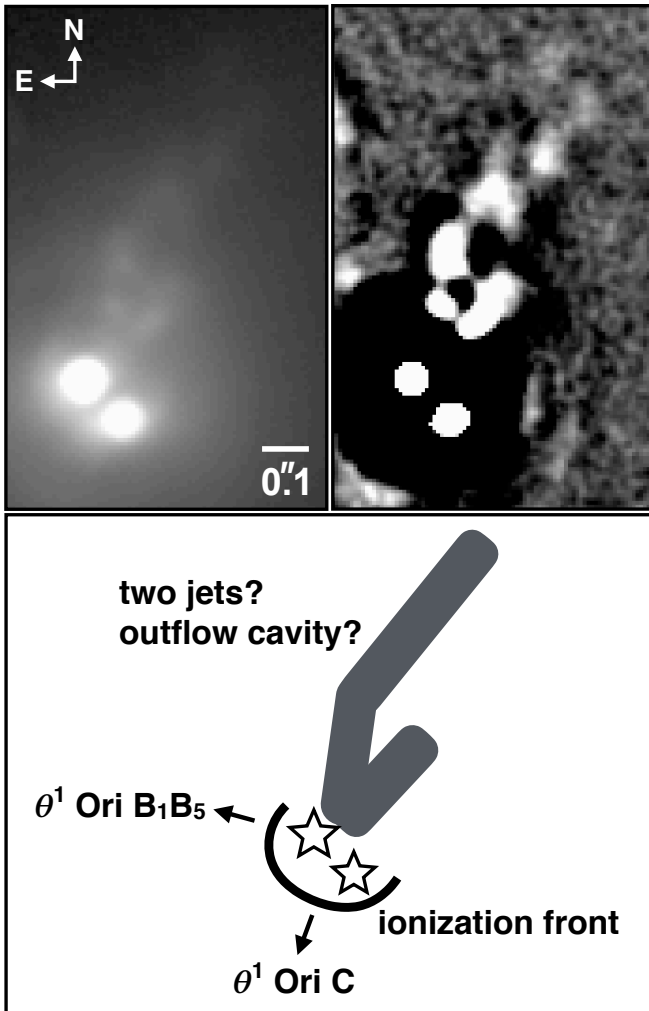


Figure 2. We bring out HH 508 by filtering out the halo of the stars with a Gaussian of FWHM = 10 pixels, and further smooth the high-pass filtered image with a two-pixel Gaussian. The east component of HH 508 has many knots and might have been bent by the wind and radiation from B₁B₅. The ionization front surrounding B₂B₃ does not directly face the nearby B₁B₅, indicating that the EUV radiation from θ^1 Ori C dominates the vicinity of B₁B₅.

still affect the morphology of proplyds even in the vicinity of θ^1 Ori B₁B₅.

The dominant role of θ^1 Ori C can be shown quantitatively by comparing the extreme UV (EUV; $\lambda < 912$ Å) fluxes from the Trapezium OB stars at the position of HH 508. Assuming all of the stars are coplanar and adopting stellar parameters from Getman et al. (2005) and Stelzer et al. (2005), we use the model spectra in Castelli & Kurucz (2004) to estimate UV luminosities and fluxes (Table 2). We find that the EUV flux ratios are A : B₁B₅ : C : D : E \approx 40 : 1 : 600 : 3 : 0.0001. θ^1 Ori C indeed dominates the EUV flux at the position of HH 508 and is responsible for illuminating the IF of B₂B₃.

The IF surrounding B₂B₃ has a radius $R_{\text{IF}} \sim 60$ au, which is smaller than the average IF radius of ~ 150 au for the 135 Orion proplyds reported in Vicente & Alves (2005). Kim et al. (2016) showed that $R_{\text{IF}} \propto \Phi^{-1/3} \dot{M}^{2/3} d^{2/3}$, where Φ is the ionizing flux, \dot{M} is the mass-loss rate, and d is the separation between the proplyd and the ionizing source. The strong ionizing flux

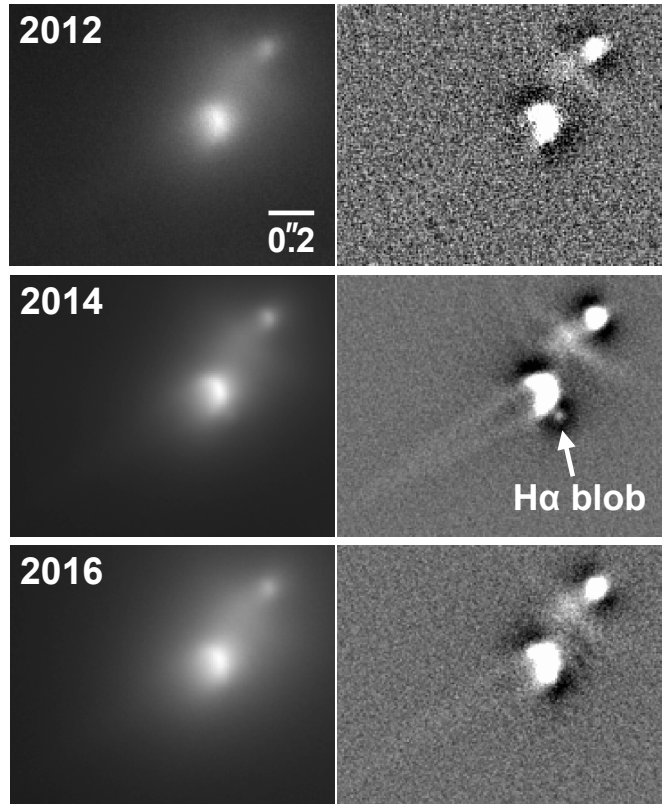


Figure 3. H α images of the binary proplyd LV 1 in different epochs. High-pass filtered images are displayed in the right panels. An H α blob emerged to the south of the major proplyd in 2014, but was not seen in the 2016 follow-up imaging. from θ^1 Ori C likely sculpted HH 508’s small IF.

3.3. LV 1 in H α

LV 1 is a binary proplyd separated by ~ 0.4 and exhibits crescent IFs and cometary tails driven by θ^1 Ori C (Figure 1). Similar to θ^1 Ori B₂B₃, both proplyds also have relatively small IFs, with $R_{\text{IF}} \sim 40$ au for the major proplyd (168–326 SE) and ~ 20 au for the minor proplyd (168–326 NW). A strip of diffuse gas between the proplyds has been interpreted as the collision of photoevaporated disk flows (Henney 2002).

In Figure 3 we present the 2012, 2014, and 2016 MagAO H α observations of LV 1. We reveal finer structure with a Gaussian kernel of FWHM = 10 pixels (bottom panels). A bright H α blob at ~ 0.13 (~ 50 au) to the south of the major proplyd appears in the 2014 image, but disappears in our 2016 observation. While its nature remains enigmatic, the blob could be an ejecta from the protostar embedded in the major proplyd. As the blob moves farther away, it disperses and fades away quickly.

We are grateful to the reviewer, John Bally, for very helpful comments. We also thank Megan Reiter for discussions. This material is based upon work supported by the National Science Foundation under grant No. 1506818 (PI Males) and NSF AAG grant No. 1615408 (PI Close). Y.-L.W. and L.M.C. are supported by the NSF AAG award and the TRIF fellowship. K.M.M.’s and L.M.C.’s work is supported by the NASA Exoplanets Research Program (XRP) by cooperative agreement NNX16AD44G. This paper includes data gathered with

the 6.5 m *Magellan* Clay Telescope at Las Campanas Observatory, Chile.

REFERENCES

- Allen, C., Costero, R., & Hernández, M. 2015, *AJ*, 150, 167
- Allen, C., Costero, R., Ruelas-Mayorga, A., & Sánchez, L. J. 2017, *MNRAS*, 466, 4937
- Bally, J., Licht, D., Smith, N., & Walawender, J. 2006, *AJ*, 131, 473
- Bally, J., O'Dell, C. R., & McCaughrean, M. 2000, *AJ*, 119, 2919
- Bally, J., & Reipurth, B. 2001, *ApJ*, 546, 299
- Bally, J., Sutherland, R. S., Devine, D., & Johnstone, D. 1998, *AJ*, 116, 293
- Castelli, F., & Kurucz, R. L. 2004, arXiv:astro-ph/0405087
- Close, L. M., Follette, K. B., Males, J. R., et al. 2014, *ApJL*, 781, L30
- Close, L. M., Males, J. R., Kopon, D., et al. 2012, *Proc. SPIE*, 8447, 84470X
- Close, L. M., Males, J. R., Morzinski, K., et al. 2013, *ApJ*, 774, 94
- Close, L. M., Wildi, F., Lloyd-Hart, M., et al. 2003, *ApJ*, 599, 537
- Eisner, J. A., Bally, J. M., Ginsburg, A., & Sheehan, P. D. 2016, *ApJ*, 826, 16
- Getman, K. V., Flaccomio, E., Broos, P. S., et al. 2005, *ApJS*, 160, 319
- Henney, W. J. 2002, *RMxAA*, 38, 71
- Johnstone, D., Hollenbach, D., & Bally, J. 1998, *ApJ*, 499, 758
- Kim, J. S., Clarke, C. J., Fang, M., & Facchini, S. 2016, *ApJL*, 826, L15
- Kounkel, M., Hartmann, L., Loinard, L., et al. 2017, *ApJ*, 834, 142
- Males, J. R., Close, L. M., Morzinski, K., et al. 2014, *ApJ*, 786, 32
- Mann, R. K., Di Francesco, J., Johnstone, D., et al. 2014, *ApJ*, 784, 82
- Mann, R. K., & Williams, J. P. 2010, *ApJ*, 725, 430
- Morzinski, K. M., Close, L. M., Males, J. R., et al. 2014, *Proc. SPIE*, 9148, 914804
- O'Dell, C. R., & Wen, Z. 1994, *ApJ*, 436, 194
- O'Dell, C. R., Wen, Z., & Hu, X. 1993, *ApJ*, 410, 696
- Petr, M. G., Du Foresto, V., Beckwith, S. V. W., Richichi, A., & McCaughrean, M. J. 1998, *ApJ*, 500, 825
- Reiter, M., Smith, N., & Bally, J. 2016, *MNRAS*, 463, 4344
- Reiter, M., Smith, N., Kiminki, M. M., & Bally, J. 2015a, *MNRAS*, 450, 564
- Reiter, M., Smith, N., Kiminki, M. M., Bally, J., & Anderson, J. 2015b, *MNRAS*, 448, 3429
- Ricci, L., Robberto, M., & Soderblom, D. R. 2008, *AJ*, 136, 2136
- Sheehan, P. D., Eisner, J. A., Mann, R. K., & Williams, J. P. 2016, *ApJ*, 831, 155
- Smith, N., Bally, J., Shuping, R. Y., Morris, M., & Kassisi, M. 2005, *AJ*, 130, 1763
- Stelzer, B., Flaccomio, E., Montmerle, T., et al. 2005, *ApJS*, 160, 557
- Tody, D. 1986, *Proc. SPIE*, 627, 733
- Tody, D. 1993, in *ASP Conf. Ser. 52, Astronomical Data Analysis Software and Systems II*, ed. R. J. Hanisch, R. J. V. Brissenden, & J. Barnes (San Francisco, CA: ASP), 173
- Vicente, S. M., & Alves, J. 2005, *A&A*, 441, 195
- Vitrichenko, É. A., & Klochkova, V. G. 2004, *Ap*, 47, 169
- Vitrichenko, É. A., Klochkova, V. G., & Tsymbal, V. V. 2006, *Ap*, 49, 96
- Windemuth, D., Herbst, W., Tingle, E., et al. 2013, *ApJ*, 768, 67
- Wu, Y.-L., Close, L. M., Males, J. R., et al. 2013, *ApJ*, 774, 45